JOURNAL OF Applied Polymer SCIENCE

Special Issue: Bioactive Surface Functionalization

Guest Editor: Prof. Koon Gee Neoh (National University of Singapore)

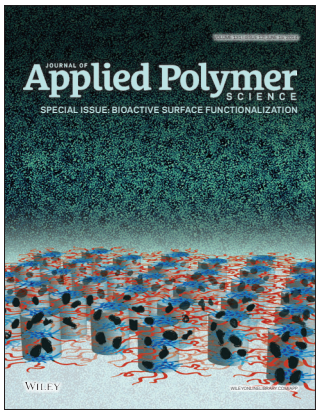

EDITORIAL

Bioactive Surface Functionalization
K. G. Neoh, *J. Appl. Polym. Sci.* 2014, **DOI: 10.1002/app.40607**

REVIEWS

Orthogonal surface functionalization through bioactive vapor-based polymer coatings
X. Deng and J. Lahann, *J. Appl. Polym. Sci.* 2014, **DOI: 10.1002/app.40315**

Surface modifying oligomers used to functionalize polymeric surfaces: Consideration of blood contact applications
M. L. Lopez-Donaire and J. P. Santerre, *J. Appl. Polym. Sci.* 2014, **DOI: 10.1002/app.40328**

Block copolymers for protein ordering
J. Malmström and J. Travas-Sejdic, *J. Appl. Polym. Sci.* 2014, **DOI: 10.1002/app.40360**

RESEARCH ARTICLES

MS-monitored conjugation of poly(ethylene glycol) monomethacrylate to RGD peptides
O. I. Bol'shakov and E. O. Akala, *J. Appl. Polym. Sci.* 2014, **DOI: 10.1002/app.40385**

Synthesis and characterization of surface-grafted poly(*N*-isopropylacrylamide) and poly(carboxylic acid)—Iron particles via atom transfer radical polymerization for biomedical applications
J. Sutrisno, A. Fuchs and C. Evrensel, *J. Appl. Polym. Sci.* 2014, **DOI: 10.1002/app.40176**

Deposition of nonfouling plasma polymers to a thermoplastic silicone elastomer for microfluidic and biomedical applications
P. Gross-Kosche, S. P. Low, R. Guo, D. A. Steele and A. Michelmore, *J. Appl. Polym. Sci.* 2014, **DOI: 10.1002/app.40500**

Regeneration effect of visible light-curing furfuryl alginate compound by release of epidermal growth factor for wound healing application
Y. Heo, H.-J. Lee, E.-H. Kim, M.-K. Kim, Y. Ito and T.-I. Son, *J. Appl. Polym. Sci.* 2014, **DOI: 10.1002/app.40113**

Bioactive agarose carbon-nanotube composites are capable of manipulating brain–implant interface
D. Y. Lewitus, K. L. Smith, J. Landers, A. V. Neimark and J. Kohn, *J. Appl. Polym. Sci.* 2014, **DOI: 10.1002/app.40297**

Preparation and characterization of 2-methacryloyloxyethyl phosphorylcholine (MPC) polymer nanofibers prepared via electrospinning for biomedical materials
T. Maeda, K. Hagiwara, S. Yoshida, T. Hasebe and A. Hotta, *J. Appl. Polym. Sci.* 2014, **DOI: 10.1002/app.40606**

Nanostructured polystyrene films engineered by plasma processes: Surface characterization and stem cell interaction
S. Mattioli, S. Martino, F. D'Angelo, C. Emiliani, J. M. Kenny and I. Armentano, *J. Appl. Polym. Sci.* 2014, **DOI: 10.1002/app.40427**

Microtextured polystyrene surfaces for three-dimensional cell culture made by a simple solvent treatment method
M. E. DeRosa, Y. Hong, R. A. Faris and H. Rao, *J. Appl. Polym. Sci.* 2014, **DOI: 10.1002/app.40181**

Elastic biodegradable starch/ethylene-co-vinyl alcohol fibre-mesh scaffolds for tissue engineering applications
M. A. Susano, I. B. Leonor, R. L. Reis and H. S. Azevedo, *J. Appl. Polym. Sci.* 2014, **DOI: 10.1002/app.40504**

Fibroblast viability and inhibitory activity against Pseudomonas aeruginosa in lactic acid–grafted chitosan hydrogels
A. Espadín, N. Vázquez, A. Tecante, L. Tamay de Dios, M. Gimeno, C. Velasquillo and K. Shirai, *J. Appl. Polym. Sci.* 2014, **DOI: 10.1002/app.40252**

Surface activity of pepsin-solubilized collagen acylated by lauroyl chloride along with succinic anhydride
C. Li, W. Liu, L. Duan, Z. Tian and G. Li, *J. Appl. Polym. Sci.* 2014, **DOI: 10.1002/app.40174**

Collagen immobilized PET-g-PVA fiber prepared by electron beam co-irradiation
G. Dai, H. Xiao, S. Zhu and M. Shi, *J. Appl. Polym. Sci.* 2014, **DOI: 10.1002/app.40597**

Journal of Applied Polymer Science

Regeneration Effect of Visible Light-Curing Furfuryl Alginate Compound by Release of Epidermal Growth Factor for Wound Healing Application

Yun Heo,[1] Hyung-Jae Lee,[1] Eun-Hye Kim,[1] Mi-Kyung Kim,[2] Yoshihiro Ito,[3] Tae-Il Son[1]

[1]Department of Systems Biotechnology, Chung-Ang University, Anseong, Gyeonggi-Do 456-756, Republic of Korea
[2]Department of Pathology, College of Medicine, Chung-Ang University, Dongjak-Gu, Seoul 156-756, Republic of Korea
[3]Nano Medical Engineering Laboratory, RIKEN, Wako, Saitama 351-0198, Japan
Correspondence to: T.-I. Son (E-mail: tisohn@cau.ac.kr)

ABSTRACT: A visible light-curable polysaccharide conjugate was prepared and was included with epidermal growth factor (EGF) for wound healing application. Alginate was modified with furfurylamine, and the furfuryl alginate (F-alginate) was mixed with Rose Bengal for visible light reactivity. The introduction of furfuryl group was confirmed by ^{1}H-NMR and UV/vis spectroscopy. Visible light-induced crosslinking was evaluated by micropatterning and weight measurement. Swelling ratio was also determined. To verify its applicability in wound healing applications, EGF was included in the system of F-alginate and Rose Bengal. After the confirmation of no cytotoxicity of F-alginate and murine EGF release from the system, cell proliferation, antibacterial activity, and animal test were performed on the system. In conclusion, it was demonstrated that the system was useful for wound healing. © 2013 Wiley Periodicals, Inc. J. Appl. Polym. Sci. **2014**, *131*, 40113.

KEYWORDS: bioengineering; biomedical applications; biomaterials; photochemistry; polysaccharides

Received 8 July 2013; accepted 23 October 2013
DOI: 10.1002/app.40113

INTRODUCTION

The skin is the largest organ in the human body. It protects the body from external stimuli or microbial infection and functions as barrier to withhold moisture. When the skin is damaged, its performance in these roles is compromised.[1] Therefore, wound healing is a dynamic process, and healing methods can be changed by wound type and healing process. However, typically a warm and moist environment is effective for wound healing, in which most healing agents are created to provide these conditions.[2,3] Because moisture is lost by evaporation at a wound site, it is very important to heal the wounds while maintaining a moist environment.[4] In addition, proper dressing adhesion is also required for wound healing.[5,6]

To promote wound healing, many materials have been developed. In particular, various natural polymers have been used as wound healing materials.[7–10] Among them, alginate has the advantages of absorbing body fluid and effectively maintaining wound site moisture.[11] In addition, alginate from seaweed is widely used in various fields, including biomedical materials because of its biocompatibility, biodegradation, and antibacterial activity.[12–14] Alginate is a linear random copolymer consisting of two monomers, α-L-glucuronic acid (G) and β-D-mannuronic acid (M) (Figure 1).[15]

Furthermore, studies using growth factors that transfer inside the cell causing cell proliferation and differentiation have been widespread.[16,17] Growth factors include different types such as epidermal growth factor (EGF), fibroblast growth factor, nerve growth factor, and transgenic growth factor.[18–21] Specifically, EGF is a growth factor that promotes cell growth, proliferation, and differentiation. EGF plays a role in wound healing and is supplied through the sweat, blood, and tissue on injury.[22] However, when the protein is injected in the body for medical application, it has been reported that EGF is inactivated due to aggregation or denaturation.[23] As a result, studies have been aimed to protect EGF functions.[24,25] In the various methods suggested to protect EGF, some studies have used chemical conjugation using crosslinking agents.[26,27] However, these methods cause risks through urea, which can affect protein denaturation.[28] To complement these problems, the photoimmobilization method has been studied, which is based on a crosslinking reaction for protein inclusion.[29] The advantages of this method are that the protein is not denatured, inclusion time is fast, and the process is simple.[30] Many photoimmobilization methods use ultraviolet (UV) light because UV light contains high-energy photons.[31] However, UV light can result in many problems such as skin cancer, immune system weakness, and genetic

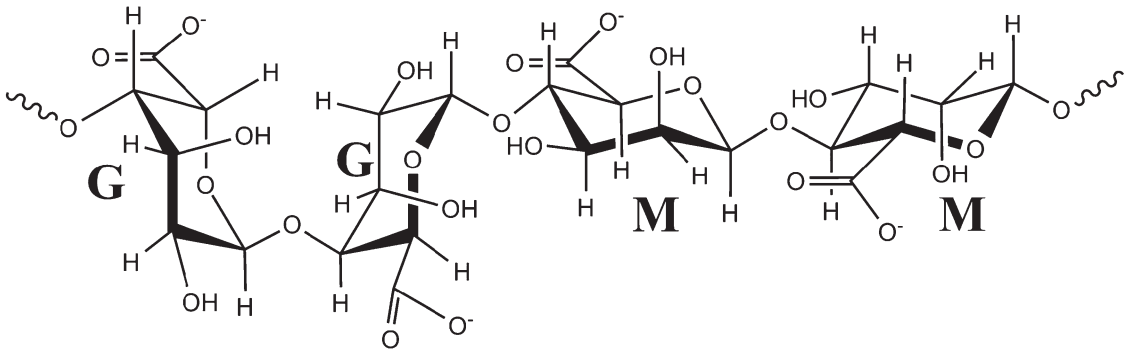

Figure 1. Alginate structure. Alginate is a linear random copolymer consisting of α-L-glucuronic acid (G) and β-D-mannuronic acid (M).

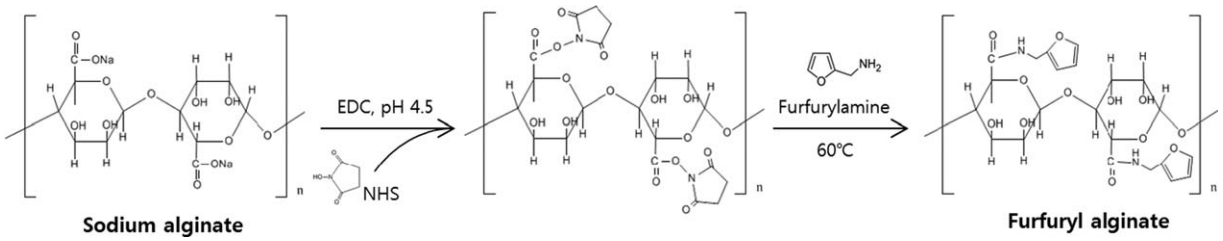

Figure 2. Preparation of F-alginate by EDC/NHS coupling.

mutation.[32,33] For these reasons, UV light is not suitable to use directly on the human body.

Therefore, in this study, we applied a photoimmobilization method using visible light that is harmless to the human body. Furfuryl alginate (F-alginate) was prepared by the introduction of a furfuryl group, which becomes a visible light-reactive group in the presence of Rose Bengal, to the alginate backbone. EGF was included in the photoreactive F-alginate system for cell proliferation. The system was also evaluated for antibacterial effect using Gram-positive bacteria *Staphylococcus aureus* and Gram-negative bacteria *Escherichia coli*. Finally, to confirm the usefulness for wound healing of EGF-included F-alginate system, we evaluated the effect in an animal model using Sprague-Dawley (SD) rats.

EXPERIMENTAL

Materials

Sodium alginate (from brown algae), *N*-(3-dimethylaminopropyl)-*N*′-ethylcarbodiimide hydrochloride (EDC), fluorescein isothiocyanate-conjugated bovine serum albumin (FITC-BSA), and furfurylamine were purchased from Sigma-Aldrich (St. Louis, MO). *N*-Hydroxysuccinimide (NHS) was purchased from Wako Pure Chemical Industries (Tokyo, Japan). Acetic acid and dimethyl sulfoxide (DMSO) were purchased from Samchun Pure Chemical Company (Seoul, Republic of Korea), and methanol was purchased from Duksan Pure Chemical Company (Seoul, Republic of Korea). Murine EGF (mEGF) was obtained from PeproTech (Rocky Hill, NJ). 3T3-L1 (mouse embryonic

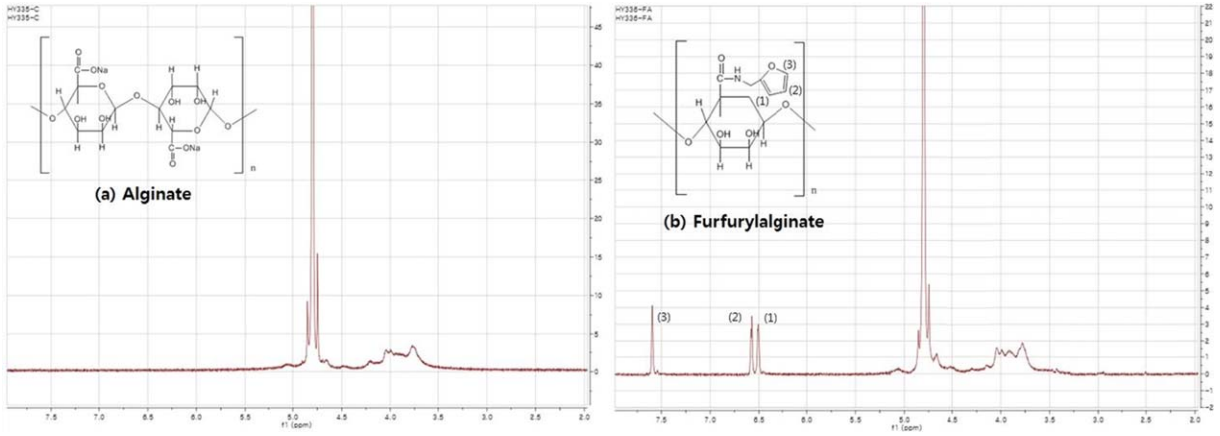

Figure 3. Comparison of 300-MHz ^{1}H-NMR spectra between (a) alginate and (b) F-alginate in deuterium oxide. According to (b), it has specific peaks at 6–8 ppm, but does not exist in alginate. These peaks are based on furan ring in furfuryl group. [Color figure can be viewed in the online issue, which is available at wileyonlinelibrary.com.]

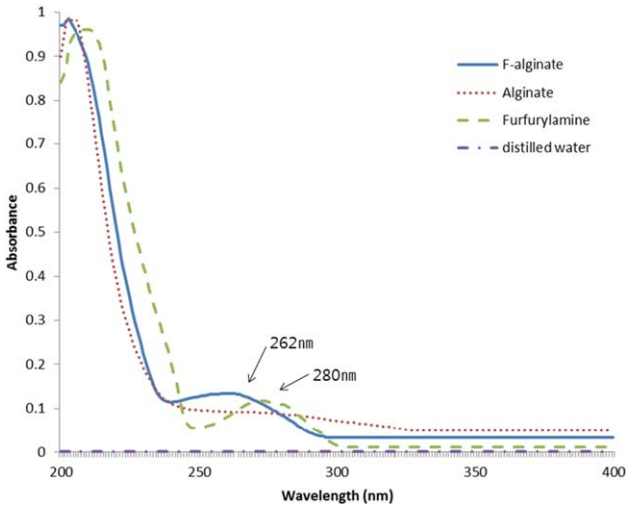

Figure 4. UV–vis absorbance values of alginate, furfurylamine, and F-alginate. [Color figure can be viewed in the online issue, which is available at wileyonlinelibrary.com.]

fibroblast cell line) cells were obtained from the Korean Cell Line Bank (Seoul, Republic of Korea). For cell culture and proliferation, Dulbecco's modified Eagle's medium (DMEM) was purchased from Wako Pure Chemical Industries, and fetal bovine serum (FBS) and penicillin–streptomycin were obtained from Gibco® (Eggenstein, Germany). For cytotoxicity test, a Cell Counting Kit-8 for water-soluble tetrazolium salt (WST) assay was procured from Dojindo (Kumamoto, Japan). For antibacterial assay, representative pathogen Gram-positive bacteria *S. aureus* (KCTC 3881) and Gram-negative bacteria *E. coli* O157: H7 (ATCC 43888) were used. To determine the wound healing effect *in vivo*, adult SD rats (7 weeks old, 200–250 g) were supplied from Samtako (Osan, Republic of Korea). For the visible light irradiation experiment, a Dr's light (visible light lamp, 420–490 nm) was obtained from Good Doctors Company (Seoul, Republic of Korea).

Preparation and Characterization of F-Alginate

To increase amide bonding efficiency between the amino group of furfurylamine and the carboxyl group of alginate, F-alginate was prepared by the previously reported EDC/NHS coupling.[34] Sodium alginate (500 mg) was dissolved in distilled water (200 mL). After that, EDC (150 mg) was added and stirred for 30 min, and then NHS (100 mg) was added. The pH of the mixtures was adjusted to pH 5 by 1 M acetic acid solution and stirred for 24 h at room temperature. Subsequently, the mixtures were filtered and evaporated. After evaporation, the mixtures were washed three times by methanol and dried under vacuum. The prepared sample was dissolved in distilled water (150 mL), and furfurylamine (200 μL) in DMSO (10 mL) was added dropwise. The mixtures were stirred at 60°C in an oil bath for 12 h. The stirred mixtures were filtered and dialyzed via dialysis membrane (cutoff: 1000 Da; Spectrum Laboratories, Rancho Dominguez, CA). After dialysis, the sample was evaporated and freeze dried. The sample was a pale yellow color. The overall reaction processes and chemical structures are illustrated in Figure 2. ^{1}H-NMR of the prepared F-alginate was determined using deuterium oxide by NMR spectrometer (Gemini 2000, 300 MHz; Varian, CA). For measurement of UV–vis absorbance values, alginate, furfurylamine, and F-alginate were measured by UV–vis spectrophotometer (T60U; Eyela, Tokyo, Japan).

Observation of Micropatterning

The prepared 0.7% F-alginate solution containing 0.1% Rose Bengal was cast on a 12-well plate and dried for 30 min at room temperature in the dark. The samples were covered with a photomask (Toppan Printing Company, Tokyo, Japan) and were irradiated using a visible light from a distance of 5 cm for 7 min. To remove nonimmobilized regions, the samples were washed by PBS and observed with a microscope (CSB-IH5; Samwon Scientific Industries, Seoul, Republic of Korea). To confirm protein immobilization, the 0.7% F-alginate solution containing FITC-BSA (5 mg/mL) was cast on a 12-well plate and air dried for 30 min at room temperature in the dark. Subsequently, the samples were irradiated using a visible light from a distance of 5 cm for 7 min and washed with PBS. The protein-immobilized and micropatterned surfaces were observed by fluorescence microscope (Eclipse TE2000-U; Nikon Sankei, Tokyo, Japan).

Crosslinking Ratio

To use the prepared F-alginate for wound healing application, optimized curing properties are necessary. For that reason, to optimize crosslinking ratio according to irradiation times and concentrations, various F-alginate samples (0.3, 0.5, 0.7, and 1%) were prepared. The samples were mixed with 0.1% Rose

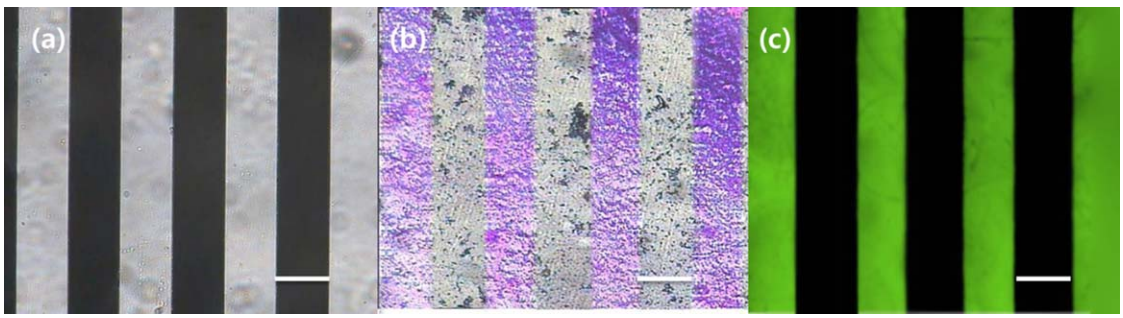

Figure 5. Micrographs of (a) micropatterned photomask and (b) photoimmobilized 0.7% F-alginate (0.1% Rose Bengal). Fluorescence micrograph of (c) photoimmobilized FITC-BSA (5 mg/mL) with 0.7% F-alginate. Images (b) and (c) show micrographs irradiated with visible light for 7 min. Scale bar, 100 μm. [Color figure can be viewed in the online issue, which is available at wileyonlinelibrary.com.]

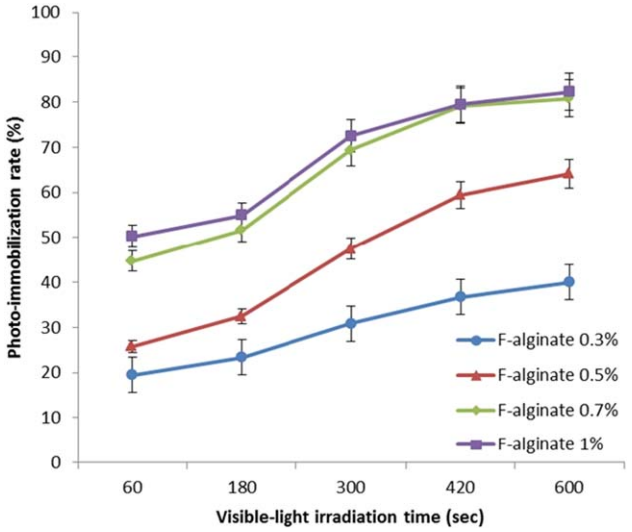

Figure 6. Ratios of crosslinking at various concentrations of F-alginate and visible light irradiation times. [Color figure can be viewed in the online issue, which is available at wileyonlinelibrary.com.]

Bengal, the mixtures (40 μL) were cast on glass microscope slide (75 mm × 25 mm; Marienfeld, Germany), and then the samples were irradiated with visible light for various times (60, 180, 300, 420, and 600 s). Subsequently, the samples were washed using PBS and weighed after drying. The crosslinking ratio was calculated as follows:

$$\text{Photocrosslinking ratio } (\%) = \frac{W_d}{W_i} \times 100,$$

where W_i is the initial sample weight, and W_d is the sample weight after washed and dried.

Swelling ratio was measured as follows. F-alginate sample (40 μL) was mixed with 0.1% Rose Bengal, and the mixture was cast on glass microscope slide and irradiated with visible light for 420 s. The photocured samples were immersed in 20 mL of distilled water and incubated at 37°C to reach equilibrium swelling state. The swelling ratio (Q) was calculated as follows:

$$\text{Swelling ratio } (Q) = \frac{W_s}{W_i} \times 100,$$

where W_s is the swollen sample weight, and W_i is the initial sample weight.

Assay of mEGF

F-alginate solutions containing 0.1% of Rose Bengal were mixed with mEGF (1 μg/mL). The mixtures were cast (30 μL) on a 24-well plate and were irradiated with visible light. The samples were incubated in PBS solution at room temperature for 72 h. The released mEGF solutions (100 μL) were added to a 96-well plate precoated with goat anti-mouse EGF antibody. After 2 h, the solutions were removed, and the wells were washed three times. Subsequently, 100 μL of the diluted detection antibody (0.5 μg/mL) was added per well and incubated at room temperature for 2 h. The diluted color development enzyme (100 μL) was added per well and incubated for 30 min. After 30 min, pink-one TMB color reagent (100 μL) was added to each well for 10 min. To stop the color reaction, the stop solution (100 μL) was added to each well. Among all reaction processes, liquids were aspirated and washed from the plate three times using washing solution. The color was measured using a microplate reader (Spectramax 190; Molecular Device, Sunnyvalve, CA) at 450 nm.

Cytotoxicity Assay

Cytotoxicity of F-alginate was measured using 3T3-L1 cells cultured in DMEM containing 1% penicillin–streptomycin and 10% FBS at 37°C in a 5% CO_2 incubator. After the cells were counted using hemocytometer (Marienfeld), the cells (3×10^4 cells per milliliter) were seeded in a 96-well plate (DK-4000 Roskilde, Kamstrupvej 90; Nunc A/S, Denmark) and incubated for 24 h to promote attachment. Various concentrations of F-alginate solution were then added to the 96-well plate. After

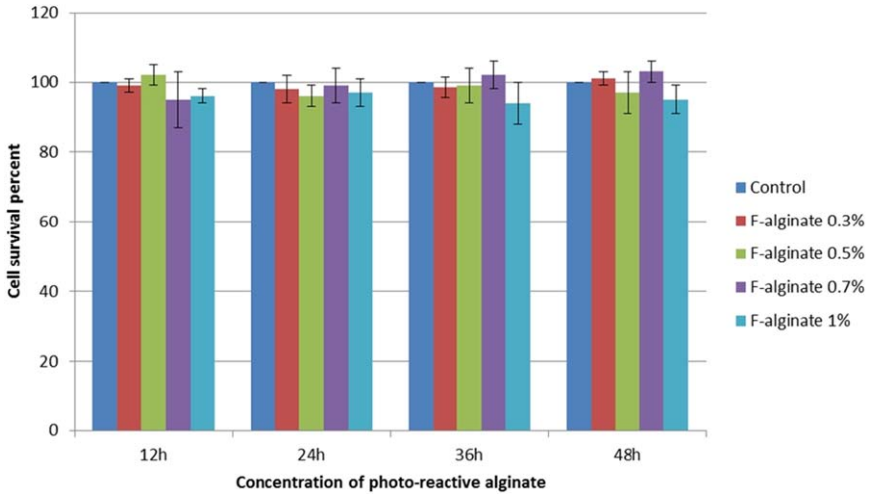

Figure 7. Cell viability assays using 3T3-L1 cells by CCK-8 kit. [Color figure can be viewed in the online issue, which is available at wileyonlinelibrary.com.]

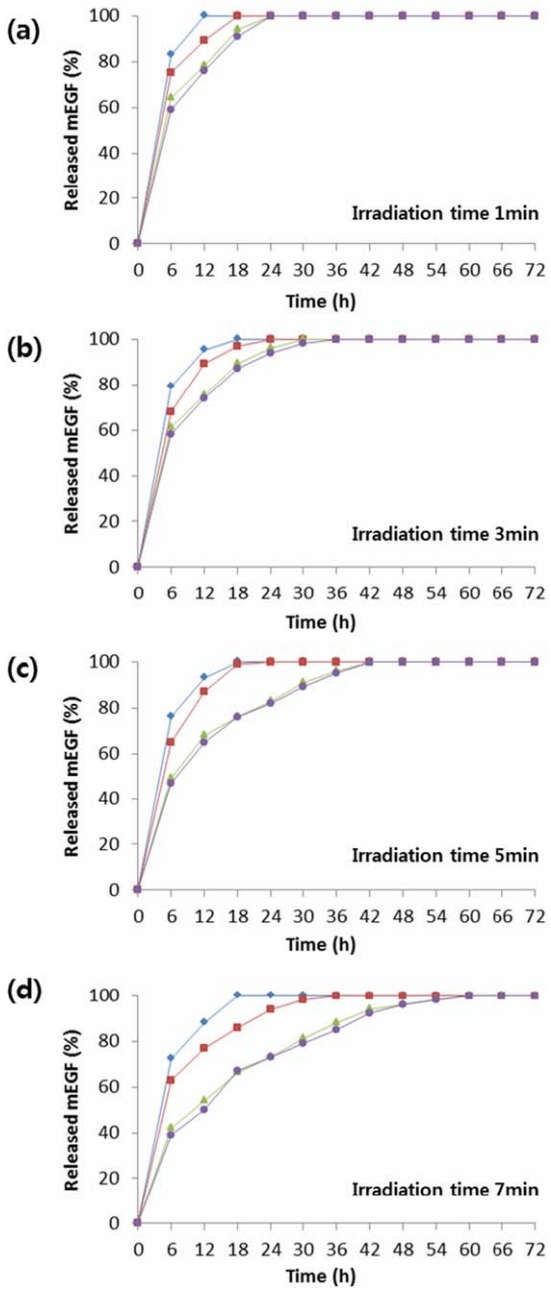

Figure 8. Time course of the *in vitro* release of mEGF under the various concentrations of F-alginate and irradiation times (1, 3, 5, and 7 min): F-alginate 0.3% (◆), F-alginate 0.5% (■), F-alginate 0.7% (▲), and F-alginate 1% (●). [Color figure can be viewed in the online issue, which is available at wileyonlinelibrary.com.]

incubation for various times (12, 24, 36, and 48 h), the media was removed, and 10% WST solution (50 μL) was added. The samples were incubated for 30 min at 37°C in a 5% CO_2 incubator and measured using a microplate reader (Spectramax 190; Molecular Devices, CA) at 450 nm.

Cell Proliferation Assay

To evaluate cell proliferation on F-alginate, 3T3-L1 cells (3×10^4 cells per well) were seeded in a 96-well plate and cultured in DMEM media containing 5% FBS for 48 h at 37°C in a 5% CO_2 incubator. At each time interval (12, 24, 36, and 48 h), the samples were washed with PBS and observed with a microscope (CSB-IH5).

In Vitro Antibacterial Assay

To measure the prepared alginate as a wound treatment, a lawn cell plate assay was analyzed to verify the antibacterial activity against pathogens. Briefly, *S. aureus* KCTC 3881 and *E. coli* O157:H7 ATCC 43888 were incubated in LB broth at 37°C. To evaluate the inhibitory activity, 10 μL of each furfurylamine, alginate solution (0.7%), and F-alginate solution (0.7%) dissolved in sterilized water were dropped onto the 6-mm-diameter disk paper and placed on a LB agar plate including 10^{6-7} CFU/mL of each cultured bacterium. The treated plates were incubated for 8 h at 37°C, and then the antibacterial activities were evaluated.

In Vivo Animal Wound Healing Test

Female SD rats, 7 months old and weighing 200–250 g, were placed in individual cages and were given sterilized water and pellet feed for experimental animals. The experimental rats were maintained at a temperature of 25°C ± 0.5°C with a 12-h light/dark cycle. The rats were anesthetized with Zoletil 50® (200 μL), and their backs were shaved and cleaned. Circular wounds with 17 mm in diameter were made in four places. Each wound was treated with 40 μL samples [Group I: control (nontreated); Group II: 0.5% Rose Bengal mixed 0.7% F-alginate solution; Group III: mEGF (50 μg/mL); and Group IV: mEGF (50 μg/mL) and 0.5% Rose Bengal mixed 0.7% F-alginate solution] and then irradiated using visible light for 7 min. After surgery, Vaseline gauzes were placed over the wounds and covered with a bandage. The dressings were changed every 3 days.

Wound tissue samples were observed via wound area measurements/visual assessment and histological examination. For visual assessment and wound area measurements, we imaged the wound, and the wound area was measured. The initial wound area was set as 100%, and for comparison, the recovered wound area was converted to a percentage.

For histological observation, the wound tissue samples were kept in 10% formalin solution at 3, 7, and 14 days after extraction. The samples were covered with paraffin and stained using hematoxylin and eosin for histological examination.

RESULTS AND DISCUSSION

Spectroscopic Characterization

In ^{1}H-NMR measurements, the resonances of F-alginate and sodium alginate are shown in Figure 3. In Figure 3(b), specific peaks corresponding to the furan ring were observed at 6.0–8.0 ppm in the ^{1}H-NMR spectrum.[35] The result indicates that a furfuryl group was introduced to alginate. The UV/vis absorbance spectra of prepared F-alginate, sodium alginate, and furfurylamine are shown in Figure 4. In Figure 4, there was no specific absorption in the sodium alginate spectrum. However, there were maximum absorptions at 280 and 262 nm corresponding to furfurylamine and F-alginate spectra, respectively. This means that F-alginate has a specific group that is analogous with furfurylamine. The reason for the absorption wavelength shift of F-alginate is based on electron delocalization

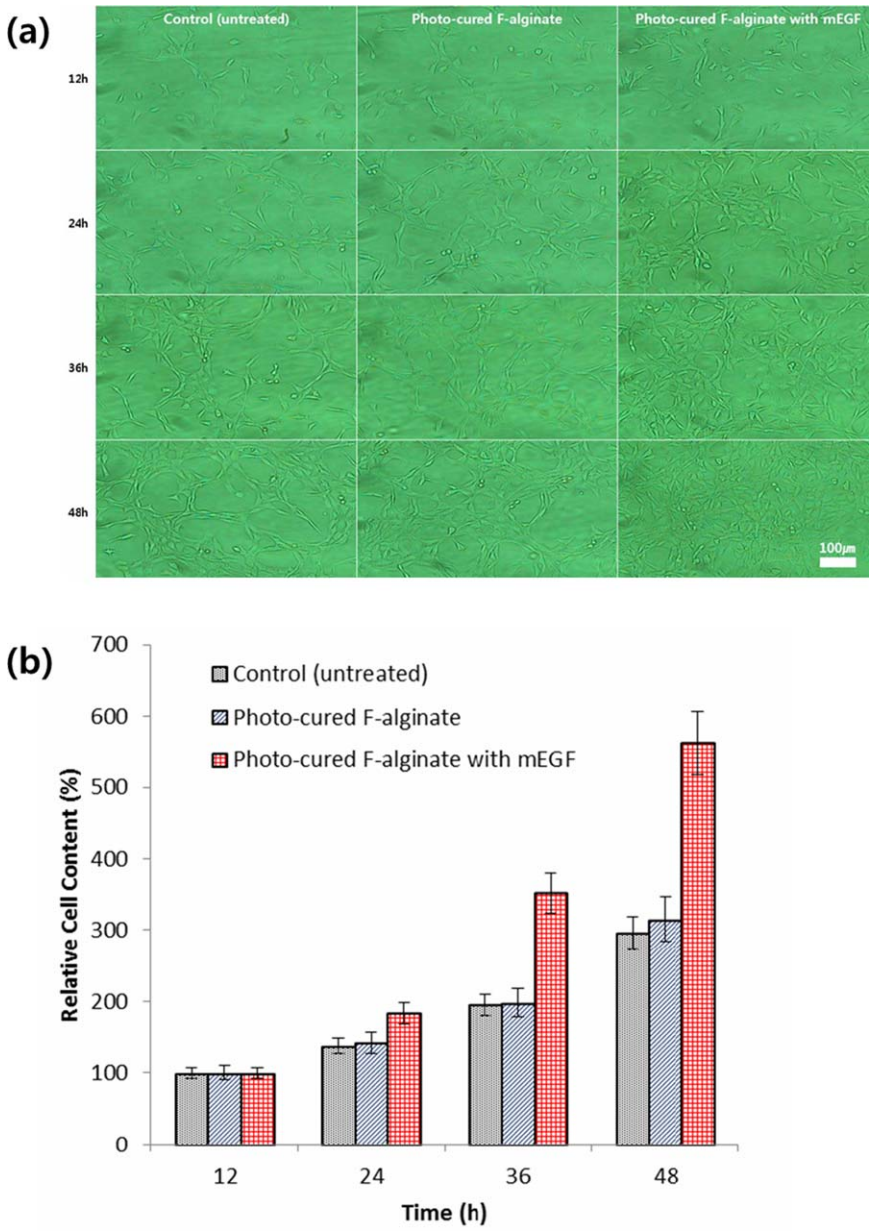

Figure 9. (a) Photographs and (b) relative cell contents of cell proliferation of fibroblasts (3T3-L1 cells) cultured on negative control (untreated), photo-cured F-alginate (0.7%), and photocured F-alginate (0.7%) with mEGF (50 μg/mL) for 12, 24, 36, and 48 h. [Color figure can be viewed in the online issue, which is available at wileyonlinelibrary.com.]

from the amide bond of modified alginate.[36] These results indicate that a furfuryl group was successfully introduced in alginate.

Micropatterning

To demonstrate the photoreactivity, micropatterning of photoreactive F-alginate was performed and is shown in Figure 5. The nonirradiated F-alginate was not observed in the micropatterning because of being washed away with distilled water. However, F-alginate was crosslinked by visible light irradiation, and the resulting surface patterning was similar to the photomask [Figure 5(b)]. These results suggest that Rose Bengal absorbs energy from visible light and then helps to generate singlet oxygen from oxygen molecules.[37] Because of the generation of singlet oxygen, furan derivatives react through the formation of furan endoperoxide. The micropattern of F-alginate solution containing FITC-BSA is shown in Figure 5(c). Using FITC-conjugated BSA, the micropattern of immobilized protein was observed by fluorescence microscope. These results suggest that visible light-curable F-alginate can be immobilized with various proteins via visible light irradiation and can be used as a wound healing agent.

Crosslinking

The crosslinking ratio of F-alginate was measured at various irradiation times and concentrations (Figure 6). When the

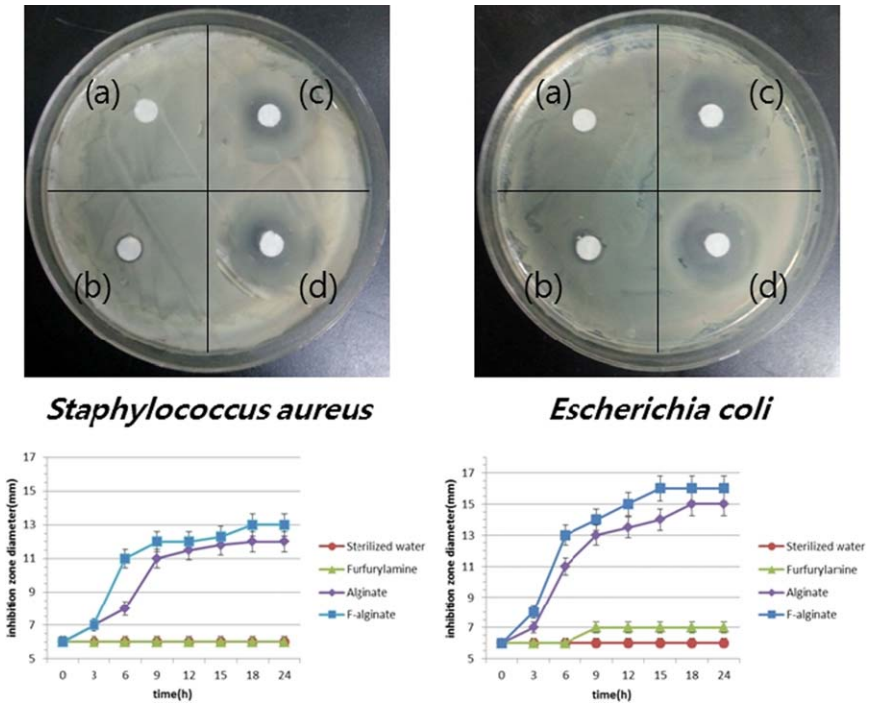

Figure 10. For antibacterial assay, the culture plates were inoculated with *Staphylococcus aureus* and *Escherichia coli* O157:H7. Type of inhibition zone: (a) sterilized water (control), (b) furfurylamine, (c) alginate, and (d) F-alginate. [Color figure can be viewed in the online issue, which is available at wileyonlinelibrary.com.]

irradiation time was 1 min, the average crosslinking ratios of samples were below 50% (0.3% F-alginate; 19%, 0.5% F-alginate; 26% and 0.7% F-alginate; 45% and 1% F-alginate; 50%). Crosslinking ratio significantly increased after 3-min irradiation time. In addition, 0.3, 0.5, 0.7, and 1% F-alginate samples showed 31, 48, 69, and 73% crosslinking ratios, respectively, for 5-min irradiation time. However, there was no significant difference in crosslinking ratio between 7- and 10-min irradiation times. Moreover, the 0.7 and 1% of crosslinking ratio were similar at the 7-min irradiation time. Generally, the crosslinking ratio was proportional to the increase in irradiation time and concentration of F-alginate. Therefore, the 7-min irradiation of visible light using 0.7% F-alginate demonstrated the most effective crosslinking ratio. The maximum swelling ratio of different concentrations of F-alginate (0.3, 0.5, 0.7, and 1%) ranged from 220 to 250%.

Cytotoxicity of F-Alginate

WST assay for cytotoxicity assay was performed, and the results are shown in Figure 7. Cell viability at various F-alginate concentrations was similar to the control group. No significant cytotoxic effects were observed for 48 h. Therefore, the prepared F-alginate is considered noncytotoxic and can be a suitable wound healing agent.

mEGF Release

Figure 8 shows the release of mEGF from crosslinked F-alginate. The release rate decreased with the increase of concentration of F-alginate, although concentrations of 0.7 and 1% had no significant difference. This result indicates that the increase of crosslinking ratio, as shown in Figure 6, contributed to the reduction of the mEGF diffusion in the crosslinked gel and that 0.7% of F-alginate was enough for inclusion of mEGF. In addition, the elongation of irradiation time also reduced the release of included mEGF. This is also considered to be related with the crosslinking behavior as shown in Figure 6.

Cell Proliferation

3T3-L1 cells were cultured under various conditions, which were negative control (untreated), photocured F-alginate, and photocured F-alginate with mEGF. Cell proliferation was checked every 12 h, and all F-alginate samples used the 0.7% concentration. In the negative control and photocured F-alginate groups, cell proliferation was slightly increased over 48 h. In these two conditions, cell proliferation was very similar. Photocured F-alginate with mEGF did not demonstrate significant changes when compared with other groups for 12 h; however, after 24 h, the rate of cell proliferation was higher than the other groups. According to Figure 9(b), the rate of cell proliferation was the highest in the photocured F-alginate with mEGF for 48 h. It means that mEGF was successfully photo-included into F-alginate and that released mEGF enhanced cell proliferation. Considering that the included mEGF was almost released from the gel, the mutagenic activity is due to the whole amount of mixed mEGF (0.5 mg/mL).

In Vitro Antibacterial Activity

The antibacterial activity of the prepared F-alginate was determined by the existence of the inhibitory zone (Figure 10). Furfurylamine showed a weak inhibitory activity against *E. coli* O157:H7, but not against *S. aureus*. Alginate and

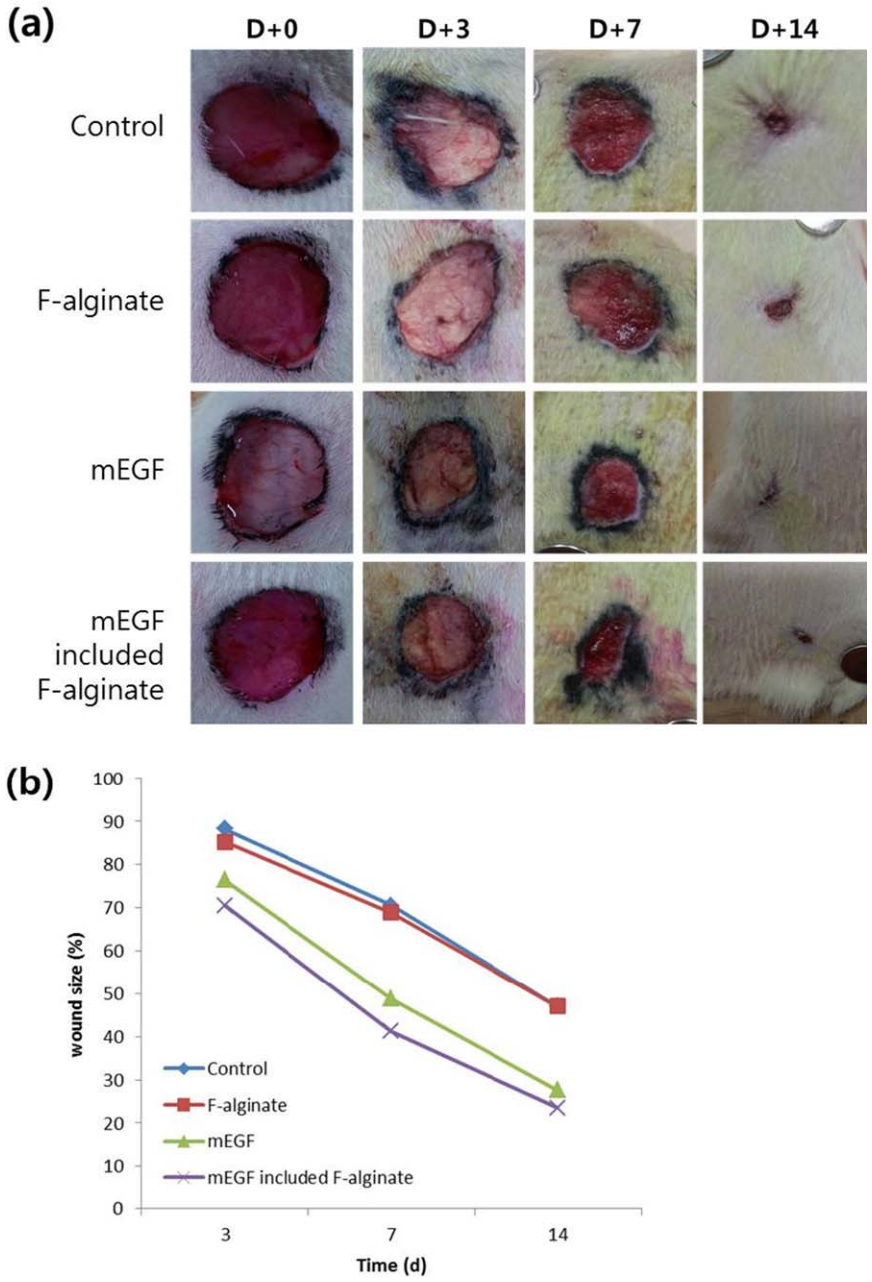

Figure 11. Visual assessment and wound area measurements. (a) Photographs of wound area at Days 3, 7, and 14 taken postoperatively after full-thickness skin excision. (b) Representative of wound area was dramatically decreased in the immobilized F-alginate with mEGF-treated group when compared with the other group. [Color figure can be viewed in the online issue, which is available at wileyonlinelibrary.com.]

F-alginate had the antibacterial activities against both pathogens, and a higher activity was shown in *E. coli* O157:H7. Furthermore, F-alginate demonstrated a stronger inhibitory activity against both pathogens. Generally, *S. aureus* is known as a Gram-positive bacterium having the thick cell wall composed of a high amount of peptidoglycan, whereas *E. coli* O157:H7, a Gram-negative bacterium, has a thicker cell membrane than Gram-positive bacteria. According to the structural difference and the impermeable cell wall of *S. aureus*, the overall antibacterial activities of those compounds showed the highest activity in *E. coli* O157:H7.

Wound Healing and Histology

To further assess the wound healing effect, an *in vivo* test was performed [Figure 11(a)]. Four control groups were set in one SD rat (Group I: Negative control; Group II: F-alginate treatment; Group III: mEGF treatment; and Group IV: mEGF-included F-alginate treatment). In visual assessment and wound area measurements, the overall wound area was decreased over 14 days. Specifically, the wound area of Group IV was the smallest when compared with the other groups, indicating that it also had the quickest recovery. As shown in Figure 11(b), the wound of Group IV recovered by 71% after 3 days and 41% after 7 days. On the

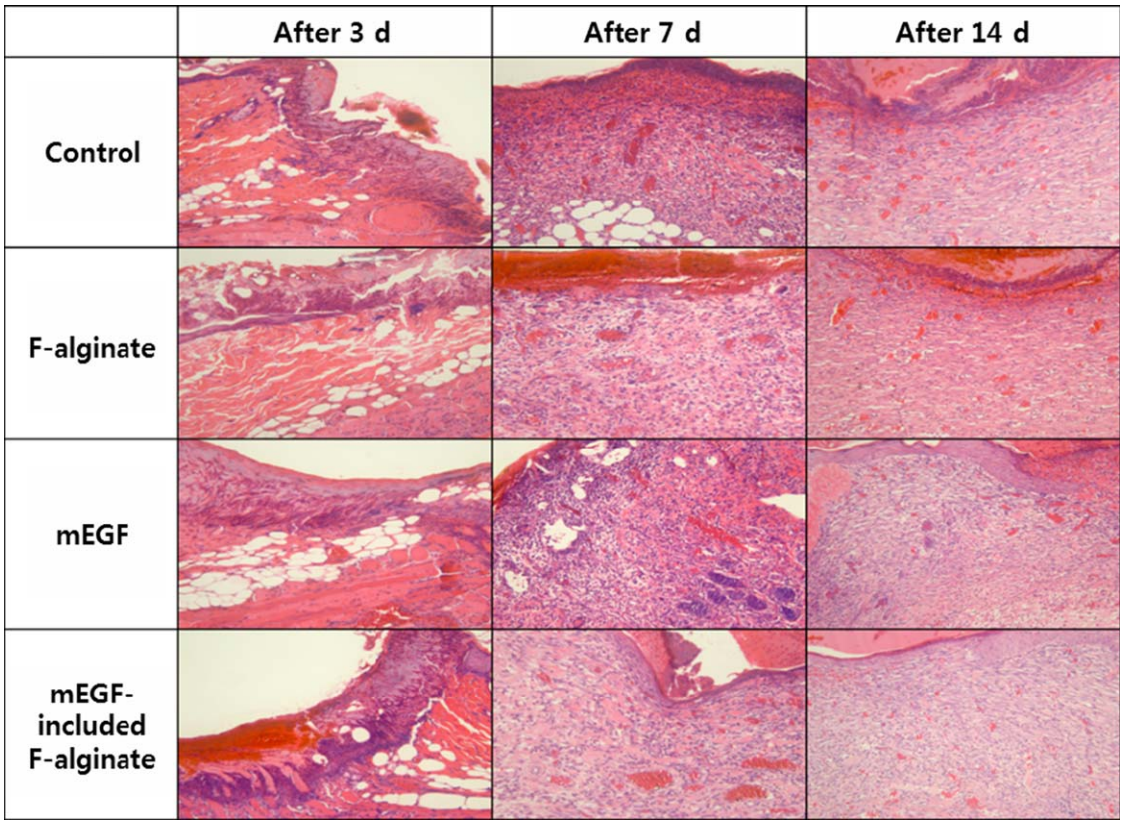

Figure 12. Histological observations of nontreated control, F-alginate, free mEGF, and F-alginate included with mEGF on the SD rat. After 3, 7, and 14 days, wounds were measured showing various effects such as inflammation, foreign body reaction, fibrosis, and epithelial regeneration by hematoxylin and eosin staining (×200). [Color figure can be viewed in the online issue, which is available at wileyonlinelibrary.com.]

Table I. Histological Results (Inflammation, Foreign Body Reaction, Fibrosis, and Epithelial Regeneration) of the Wound Area After Treatments

	Control	F-alginate	mEGF	mEGF-included F-alginate
		After 3 days		
Inflammation	3	3	3	3
Foreign body reaction	0	0	0	0
Fibrosis	0	0	0	0
Epithelial regeneration	0	0	0	0
		After 7 days		
Inflammation	3	1	2	1
Foreign body reaction	2	1	2	1
Fibrosis	0	0	0	1
Epithelial regeneration	0	1	1	2
		After 14 days		
Inflammation	3	1	1	0
Foreign body reaction	2	0	1	0
Fibrosis	1	2	2	3
Epithelial regeneration	1	3	3	3

Point meaning: 1: below 1/3 of the whole wound; 2: below 2/3 of the whole wound; 3: in the whole wound. (In inflammation and foreign body reaction, 3 point meaning is severe condition. In epithelial regeneration and fibrosis, 3 point meaning is completely healed.)

14th day after surgery, the wound showed the best healing condition, which was 24%. These results indicate that mEGF-included F-alginate was more effective than free mEGF.

Figure 12 shows the histological result (inflammation, foreign body reaction, fibrosis, and epithelial regeneration) of the wound area, and the results are summarized in Table I. Neither fibrosis nor epithelial regeneration was observed in all the groups until 3 days after operation. On the seventh day postoperation, Group I still showed severe inflammation/foreign body reaction and did not show epithelial regeneration. Groups II and III showed inflammation/foreign body reaction and started epithelial regeneration. Group IV showed low inflammation/foreign body reaction and better epithelial regeneration than the other groups. On the 14th day postoperation, Group I showed sustained inflammation/foreign body reaction and did not show complete epithelial regeneration. Fibrosis only occurred in some parts. Group II showed inflammation/epithelial regeneration; however, fibrosis did not occur completely. Group III showed slight inflammation/foreign body reaction and was good epithelial regeneration. However, fibrosis did not occur completely. Group IV did not show inflammation/foreign body reaction, and epithelial regeneration/fibrosis occurred completely. These results indicate that mEGF-included F-alginate system had a well-preserved wound healing effect after protein inclusion.

CONCLUSION

Alginate modified with a furfuryl group was prepared for wound dressing with enhanced healing efficacy. It is expected that F-alginate helps in wound healing by offering antibacterial activity and a moist environment to reduce initial inflammation. In addition, F-alginate could include proteins like mEGF, and it is more effective for wound healing by promoting cell growth, proliferation, and differentiation. Therefore, photocrosslinked F-alginate with mEGF, which has a high biocompatibility, is an ideal biomaterial for wound healing.

ACKNOWLEDGMENTS

This research was supported by the Chung-Ang University Research Scholarship Grants in 2013.

REFERENCES

1. Wilson, S. E.; Netto, M.; Ambrósio, R. *Am. J. Ophthalmol.* **2003**, *136*, 530.
2. Eaglstein, W. H.; Mertz, P. M. *J. Invest. Dermatol.* **1978**, *71*, 382.
3. Wang, P.; Samji, N. *Org. Coat. Plast. Chem.* **1980**, *42*, 628.
4. Kokabi, M.; Sirousazar, M.; Hassan, Z. M. *Eur. Polym. J.* **2007**, *43*, 773.
5. Reddy, T. T.; Kano, A.; Maruyama, A.; Hadano, M.; Takahara, A. *Biomacromolecules* **2008**, *9*, 1313.
6. Tanodekaew, S.; Prasitsilp, M.; Swasdison, S.; Thavornyutikarn, B.; Pothsree, T.; Pateepasen, R. *Biomaterials* **2004**, *25*, 1453.
7. Azad, A. K.; Sermsintham, N.; Chandrkrachang, S.; Stevens, W. F. *J. Biomed. Mater. Res. Part B: Appl. Biomater.* **2004**, *69*, 216.
8. Kickhöfen, B.; Wokalek, H.; Scheel, D.; Ruh, H. *Biomaterials* **1986**, *7*, 67.
9. Tavaria, F.; Jorge, M.; Marchetti, G.; Souza, V.; Ruiz, A.; Malcata, F.; Pintado, M.; Carvalho, J. *New Biotechnol.* **2009**, *25*, S10.
10. Kirker, K. R.; Luo, Y.; Nielson, J. H.; Shelby, J.; Prestwich, G. D. *Biomaterials* **2002**, *23*, 3661.
11. Balakrishnan, B.; Mohanty, M.; Umashankar, P.; Jayakrishnan, A. *Biomaterials* **2005**, *26*, 6335.
12. Mikołajczyk, T.; Wołowska-Czapnik, D. *Fibres Text. Eastern Eur.* **2005**, *3*, 35.
13. De Vos, P.; De Haan, B.; Van Schilfgaarde, R. *Biomaterials* **1997**, *18*, 273.
14. Bouhadir, K. H.; Lee, K. Y.; Alsberg, E.; Damm, K. L.; Anderson, K. W.; Mooney, D. J. *Biotechnol. Prog.* **2008**, *17*, 945.
15. Lee, K. Y.; Park, W. H.; Ha, W. S. *J. Appl. Polym. Sci.* **1997**, *63*, 425.
16. Brown, L. F.; Yeo, K. T.; Berse, B.; Yeo, T. K.; Senger, D. R.; Dvorak, H. F.; Van De Water, L. *J. Exp. Med.* **1992**, *176*, 1375.
17. Imanishi, J.; Kamiyama, K.; Iguchi, I.; Kita, M.; Sotozono, C.; Kinoshita, S. *Prog. Retin. Eye Res.* **2000**, *19*, 113.
18. Janet, T.; Lüdecke, G.; Otten, U.; Unsicker, K. *J. Neurosci. Res.* **2004**, *40*, 707.
19. Derynck, R.; Zhang, Y. E. *Nature* **2003**, *425*, 577.
20. Meyer, M.; Matsuoka, I.; Wetmore, C.; Olson, L.; Thoenen, H. *J. Cell Biol.* **1992**, *119*, 45.
21. Niswander, L.; Martin, G. *Development* **1992**, *114*, 755.
22. Jun, H. W.; West, J. *J. Biomater. Sci. Polym. Ed.* **2004**, *15*, 73.
23. Costantino, H. R.; Langer, R.; Klibanov, A. M. *J. Pharm. Sci.* **1994**, *83*, 1662.
24. Ogiwara, K.; Nagaoka, M.; Cho, C. S.; Akaike, T. *Biotechnol. Lett.* **2005**, *27*, 1633.
25. Hou, K.; Zaniewski, R.; Roy, S. *Biotechnol. Appl. Biochem.* **1991**, *13*, 257.
26. Sun, W. Q.; Davidson, P.; Chan, H. S. O. *Biochim. Biophys. Acta—Gen. Subj.* **1998**, *1425*, 245.
27. Sano, S.; Kato, K.; Ikada, Y. *Biomaterials* **1993**, *14*, 817.
28. Bennion, B. J.; Daggett, V. *Proc. Natl. Acad. Sci. USA* **2003**, *100*, 5142.
29. Ito, Y.; Nogawa, M. *Biomaterials* **2003**, *24*, 3021.
30. Chen, G.; Ito, Y.; Imanishi, Y. *Biochim. Biophys. Acta—Mol. Cell Res.* **1997**, *1358*, 200.
31. Hazer, B.; Demirel, S. I.; Borcakli, M.; Eroglu, M. S.; Cakmak, M.; Erman, B. *Polym. Bull.* **2001**, *46*, 389.
32. Kvam, E.; Tyrrell, R. M. *Carcinogenesis* **1997**, *18*, 2379.
33. Bochow, T. W.; West, S. K.; Azar, A.; Munoz, B.; Sommer, A.; Taylor, H. R. *Arch. Ophthalmol.* **1989**, *107*, 369.
34. Lomant, A. J.; Fairbanks, G. *J. Mol. Biol.* **1976**, *104*, 243.
35. Alvarez-Ibarra, C.; Quiroga-Feijóo, M. L.; Toledano, E. *J. Chem. Soc. Perkin Trans. 2* **1998**, 679.
36. Barr, J.; Wallon, S. *J. Appl. Polym. Sci.* **2003**, *15*, 1079.
37. Son, T. I.; Sakuragi, M.; Takahashi, S.; Obuse, S.; Kang, J.; Fujishiro, M.; Matsushita, H.; Gong, J.; Shimizu, S.; Tajima, Y., Ito, Y. *Acta Biomater.* **2010**, *6*, 4005.